ENVIRONMENTAL RESEARCH
LETTERS

LETTER

Seasonality of inundation in geographically isolated wetlands across the United States

Junehyeong Park[1] ⓘ, **Mukesh Kumar**[1,*] ⓘ, **Charles R Lane**[2] **and Nandita B Basu**[3]

1 Department of Civil, Construction and Environmental Engineering, University of Alabama, Tuscaloosa, AL, United States of America
2 US Environmental Protection Agency, Office of Research and Development, Cincinnati, OH, United States of America
3 Department of Civil and Environmental Engineering, University of Waterloo, Waterloo, ON, Canada
* Author to whom any correspondence should be addressed.

E-mail: mukesh.kumar@ua.edu

Abstract

Inundation area is a major control on the ecosystem services provisioned by geographically isolated wetlands. Despite its importance, there has not been any comprehensive study to map out the seasonal inundation characteristics of geographically isolated wetlands over the continental United States (CONUS). This study fills the aforementioned gap by evaluating the seasonality or the long-term intra-annual variations of wetland inundation in ten wetlandscapes across the CONUS. We also assess the consistency of these intra-annual variations. Finally, we evaluate the extent to which the seasonality can be explained based on widely available hydrologic fluxes. Our findings highlight significant intra-annual variations of inundation within most wetlandscapes, with a standard deviation of the long-term averaged monthly inundation area ranging from 15% to 151% of its mean across the wetlandscapes. Stark differences in inundation seasonality are observed between snow-affected vs. rain-fed wetlandscapes. The former usually shows the maximum monthly inundation in April following spring snowmelt (SM), while the latter experiences the maximum in February. Although the magnitude of inundation fraction has changed over time in several wetlandscapes, the seasonality of these wetlands shows remarkable constancy. Overall, commonly available regional hydrologic fluxes (e.g. rainfall, SM, and evapotranspiration) are found to be able to explain the inundation seasonality at wetlandscape scale with determination coefficients greater than 0.57 in 7 out of 10 wetlandscapes. Our methodology and presented results may be used to map inundation seasonality and consequently account for its impact on wetland functions.

1. Introduction

Wetlands provide a multitude of ecosystem services (Mitsch and Gosselink 2000, Bullock and Acreman 2003, Zhu *et al* 2017), including groundwater recharge (McCarthy 2006, Freitas *et al* 2019, Wossenyeleh *et al* 2021), flood control (Hey and Philippi 1995, Watson *et al* 2016, Thorslund *et al* 2017), methane emission (Bloom *et al* 2017, Zhang *et al* 2017, Hondula *et al* 2021), storage (Lane and D'Amico 2010), provisioning of habitat for aquatic plants and animals (Knight *et al* 2001, Zedler and Kercher 2005, Benson *et al* 2018), and water quality buffering (Gilliam 1994, Sawatzky and Fahrig

2019) through the removal of carbon (Reuter *et al* 1992, Baptista *et al* 2003, Kayranli *et al* 2010), metals (Mungur *et al* 1995, Marchand *et al* 2010, Schück and Greger 2020, Sarkar *et al* 2021), sediments (Jordan *et al* 2003, Liu *et al* 2019, Wang *et al* 2019), and nitrate (Lin *et al* 2002, Golden *et al* 2017, Cheng *et al* 2020). Geographically Isolated Wetlands or GIWs (Tiner 2003a, Mushet *et al* 2015) are a specific subset of wetland systems that also provide the aforementioned services (Marton *et al* 2015, Calhoun *et al* 2017, Cheng and Basu 2017, Lane *et al* 2018), but have unfortunately been accorded limited protections (Creed *et al* 2017). This is partly because these wetlands are completely surrounded by uplands, and

so they do not seem to be connected to other wetlands or waterbodies through a well-defined surface water connection, resulting in them being left out of jurisdictional reach. However, these wetlands can have hydrological connections with other waterbodies via subsurface flow or groundwater or may even have temporary surface water connections (Tiner 2003b).

The functions provided by GIWs are often related to their inundation characteristics (Melton *et al* 2013, Cohen *et al* 2016, Cheng and Basu 2017). The majority of the studies that quantify ecosystem services provisioned by wetlands (Bloom *et al* 2017, Zhang *et al* 2017, Hill *et al* 2018, Holmquist *et al* 2018) use a fixed area, which is often derived from National Wetlands Inventory (NWI) (U.S. Fish and Wildlife Service 2019) or other similar databases. This is despite the fact that wetlands exhibit intra-annual and interannual dynamics in their inundation characteristics, which in turn is bound to affect the services offered by them. While several recent studies have attempted to map regional wetland inundation and changes in it over the years (Huang *et al* 2014, Halabisky *et al* 2016, Jin *et al* 2017, Wu *et al* 2019), there has not been any comprehensive study to map out the seasonality of inundation for the primary wetlandscapes in the continental United States (CONUS).

This study addresses the aforementioned need by deriving the seasonality of GIWs across the CONUS for the first time. We also assess the change in seasonality over the analysis period. Consistency of the seasonality, i.e. the recurrence frequency of wet and dry months, is also evaluated. Finally, we estimate the degree to which the inundation seasonality can be explained based on monthly regional hydroclimatic forcings. To these ends, section 2 provides details of study sites and the method to delineate the time-series of the inundated area of GIWs. Section 3 presents the results regarding the seasonality of inundated areas of GIWs, its consistency, and meteorological controls on it. Section 4 summarizes the major results and conclusions, discusses the limitations, and suggests future research directions.

2. Data and methods

2.1. Data used to map wetland inundation
Remote sensing provides the opportunity to map spatio-temporal variations in wetland extent over large regions. Several efforts have been made in this regard, especially at local scales (Wu and Lane 2016, Hird *et al* 2017, Kaplan and Avdan 2018, Rezaee *et al* 2018, Wu *et al* 2019). Recently, the Global Surface Water (GSW; Pekel *et al* 2016) and Dynamic Surface Water Extent (DSWE; Jones 2015, 2019) maps have been used to study inundation dynamics (Allen and Pavelsky 2018, Luijendijk *et al* 2018, Mentaschi *et al* 2018). Here, we used the GSW inundation data from March 1985 to October 2015 to map the seasonality of inundated areas of GIWs. GSW was used here as

it provides the opportunity to extend the methodology to other places beyond the CONUS. In addition, it is easy to use, and provides an estimate of inundation for each pixel within a month. The GSW v1.0 data was downloaded using the Google Earth Engine.
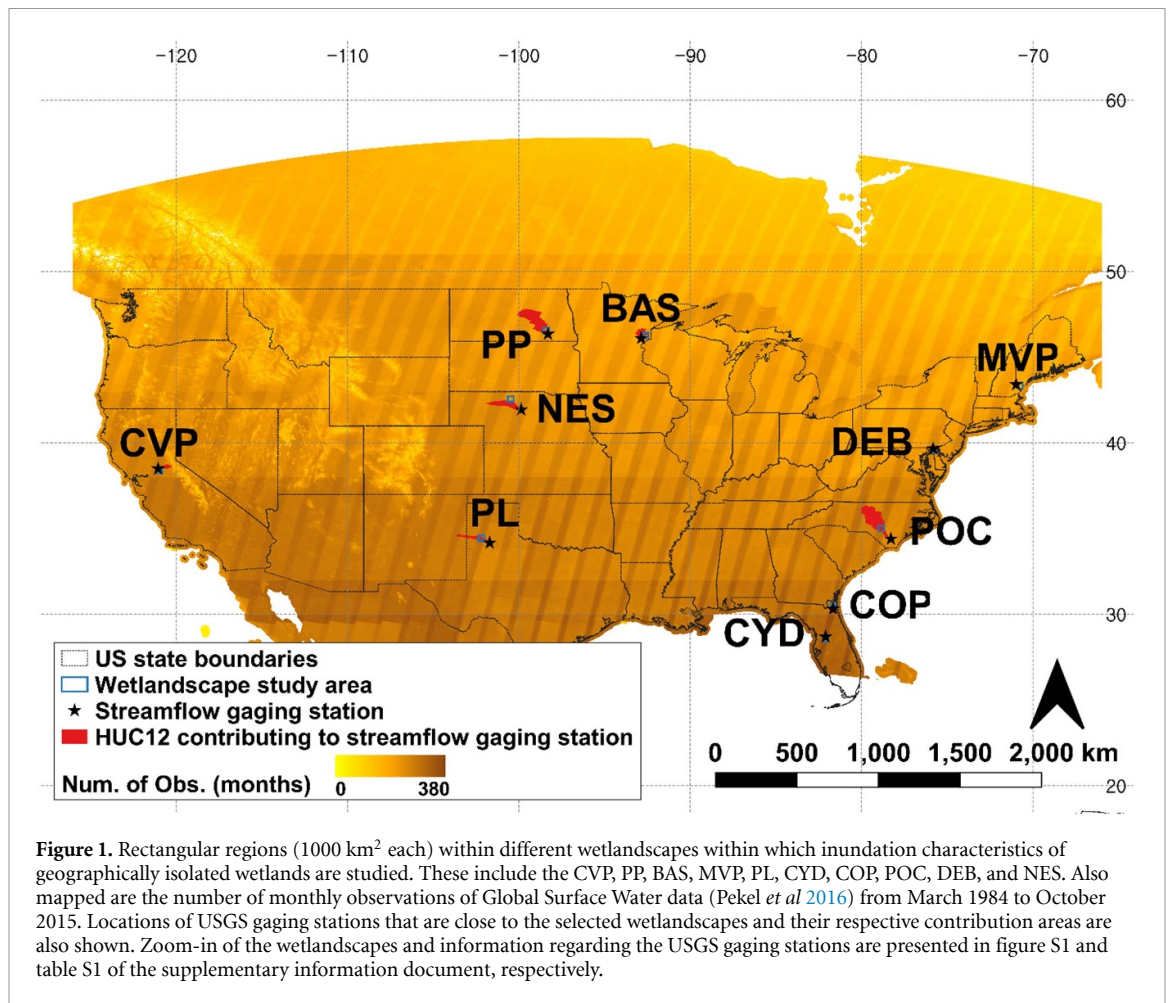
2.2. Selection of study sites
We studied the inundation characteristics in ten large wetlandscapes of the CONUS (figure 1). These include the California vernal pools (CVP), Prairie potholes (PP), Basin wetlands (BAS), Maine vernal pools (MVP), Playa lakes (PL), Cypress domes (CYD), Coastal plain wetlands (COP), Pocosins (POC), Delmarva bays (DEB), and Nebraska Sandhills (NES). Inundation characteristics were assessed within a selected rectangular region of 1000 km^2 area at each wetlandscape. The location of the rectangular region within each wetlandscape was determined based on the following heuristic: (a) wetlandscape locations were first identified based on the Cohen *et al* (2016) and Tiner (2003b), (b) within each wetlandscapes, locations with a high density of wetlands based on NWI data were subset, (c) from these subsets, locations with little or infrequent gaps in GSW data were identified, (d) rectangular regions with a long-term (>5 years, figure S1 and table S1 available online at stacks.iop.org/ERL/17/054005/mmedia) USGS discharge gaging station nearby for which the contribution area largely lies in the wetlandscape, were preferred. Post-processing of inundation data (figure S7) shows that the shape index or the ratio of the total square root of wetland area to total wetland perimeter in many of these landscapes have changed during the analysis period, thus indicating anthropogenic influences (Van Meter and Basu 2015, Krapu *et al* 2018).

2.3. Hydroclimatic data
To assess the role of hydroclimatic fluxes on the seasonality of GIWs' inundation area, monthly forcings data such as rainfall, SM, evapotranspiration (ET), and potential evapotranspiration (PET) were obtained from the NLDAS-2 data set (Xia *et al* 2012). The majority of these fluxes have been validated in a range of settings (Luo *et al* 2003, Pan *et al* 2003, Nan *et al* 2010, Nearing *et al* 2016) and has been used extensively in hydrologic studies (Mitchell *et al* 2004, Yu *et al* 2013, Maxwell *et al* 2015, Wang *et al* 2018, Zhang *et al* 2019). Data were extracted for all NLDAS-2 grids that intersected with 1000 km^2 study region within each wetlandscape. Records corresponding to each wetlandscape were spatially averaged.

2.4. Identifying GIWs from NWI
GIWs were derived within the selected rectangular regions. To this end, we used a method similar to the one presented in Lane and D'Amico (2016). The method involves using the NWI and National Hydrographic Dataset (NHD). To select GIWs from

Figure 1. Rectangular regions (1000 km² each) within different wetlandscapes within which inundation characteristics of geographically isolated wetlands are studied. These include the CVP, PP, BAS, MVP, PL, CYD, COP, POC, DEB, and NES. Also mapped are the number of monthly observations of Global Surface Water data (Pekel *et al* 2016) from March 1984 to October 2015. Locations of USGS gaging stations that are close to the selected wetlandscapes and their respective contribution areas are also shown. Zoom-in of the wetlandscapes and information regarding the USGS gaging stations are presented in figure S1 and table S1 of the supplementary information document, respectively.

NWI, first riverine, marine, and estuarine wetland systems were excluded from the NWI, i.e. only the palustrine and lacustrine wetlands were considered for further analysis. Next, NHD data that includes hydrographic features such as rivers, lakes, reservoirs, wetlands, and oceans was used. Following Lane and D'Amico (2016), we obtained 10 m buffer polygons for rivers, NHD lakes larger than 8 ha, other water bodies (e.g. reservoirs, playa, etc) larger than 1.5 ha, and all other flowlines and area features (including bays/inlets, locks, levees, etc.). Palustrine and lacustrine wetland polygons, selected above from NWI, that intersect with the 10 m buffered NHD polygons were then removed, as they were considered to have surficial connections with other waterbodies. The remaining wetlands were termed as GIWs. The resulting extracted wetlands (figure 2) were the considered GIWs for ensuing analyses.

2.5. Delineating the dynamics of GIWs

To evaluate GIW dynamics, first, the maximum extent of GIWs was derived from the GSW maps. To this end, a multi-step process was followed (figure 3). By counting all the water pixels in GSW data within a wetlandscape, the inundation area for every month from March 1984 to October 2015 was evaluated. From this, the wettest month during the analysis period, characterized by the maximum inundation area within a wetlandscape, was identified. For the wettest month in the GSW map, we then distinguished wet pixels into GIWs and non-GIWs. Non-GIWs were the contiguous wet pixels that touched or intersected with water bodies that are not classified as GIWs in the NWI data (identified in section 2.4) or, in other words, water bodies that are termed as NWI → other waterbodies in figure 2. If contiguous wet pixels did not touch any GIWs in the NWI data (or NWI → GIWs in figure 2), these pixels were classified as non-GIWs as they are likely to be either non-GIW wetlands or ephemeral pondings or misclassifications in the satellite data. It is also possible that commission errors were also due to poorer data resolution and inconsistent mapping protocol of older NWI data (Tiner 1997, Wu and Lane 2017), as we assumed the NWI to be the most accurate baseline dataset for these analyses. The rest of the wet pixels in the GSW map were identified as GIWs. Each contiguous wet pixel region was considered a GIW henceforth. The derived map represented the maximum extent of selected GIWs during the analyses period. It is to be noted that there is a possibility that the identified extent may not be the absolute maximum extent of the selected GIWs in reality, as the analyses could only be performed for the dates for which GSW data exists.
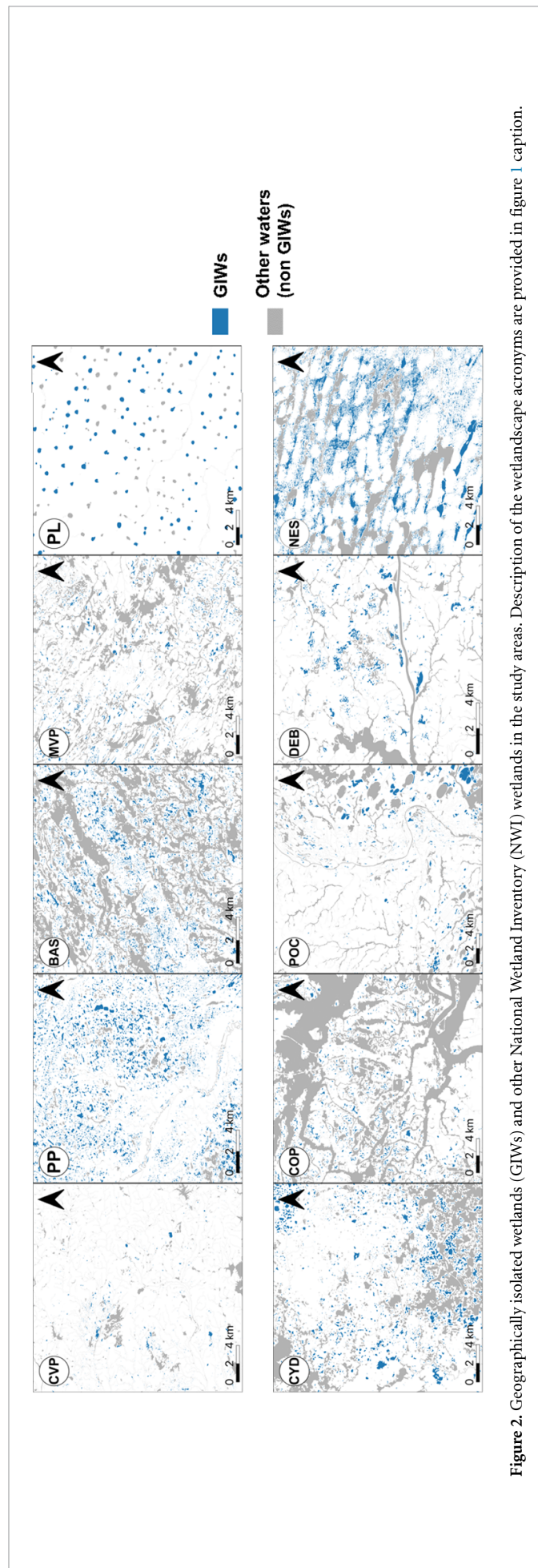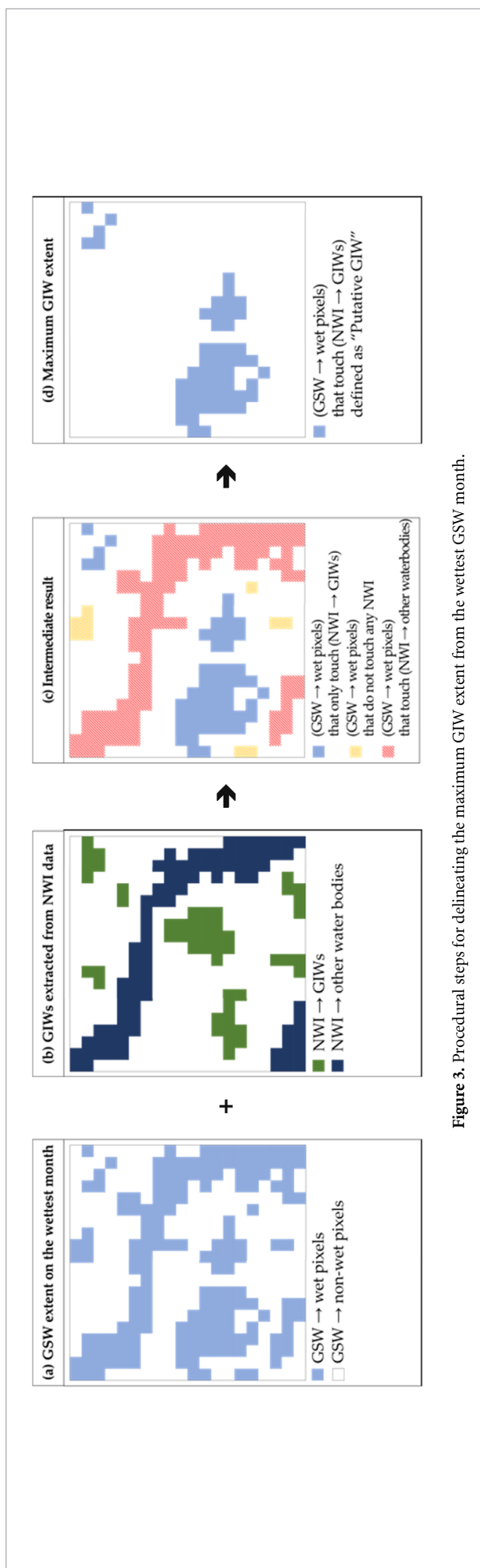
Figure 2. Geographically isolated wetlands (GIWs) and other National Wetland Inventory (NWI) wetlands in the study areas. Description of the wetlandscape acronyms are provided in figure 1 caption.

Figure 3. Procedural steps for delineating the maximum GIW extent from the wettest GSW month.

The maximum extent of GIWs, extracted above was then used to obtain the temporal dynamics. To this end, for each GIW, the inundation area was evaluated for all months, with no-data values being less than 5% of the maximum extent area. When no-data pixels exceeded 5% of the maximum extent area of a given GIW for a given timestep, the record was neglected. Next, the inundation area fraction (IAF) of a GIW was calculated as the ratio of the wet pixel area in a given timestep divided by the all-time maximum wet pixel area of the GIW. The IAF varies from 0 to 1, thus providing a standardized inundation fraction for GIWs. IAF equal to zero indicates a completely dry GIW or a GIW with no water detected within it. A value of one indicates its maximum extent. For many GIWs, the minimum is greater than zero, indicating that those GIWs do not fully dry up. During wet periods, it is expected that individual GIWs will have larger IAFs. Next, the average IAF for a given month overall GIWs within each wetlandscape, hereafter called allGIW_IAF, was obtained. Finally, mean monthly allGIW_IAF (allGIW_IAF$_m$ hereafter) and monthly standard deviation of allGIW_IAF (allGIW_IAF$_{std}$ hereafter) were evaluated. In other words, a single allGIW_IAF$_m$ for January was obtained based on allGIW_IAF estimates from all January months in the data period. The intra-annual variation in allGIW_IAF$_m$ indicates the seasonality of GIW dynamics within a wetlandscape, while allGIW_IAF$_{std}$ provides a measure of inter-annual variations in averaged monthly inundation fractions.

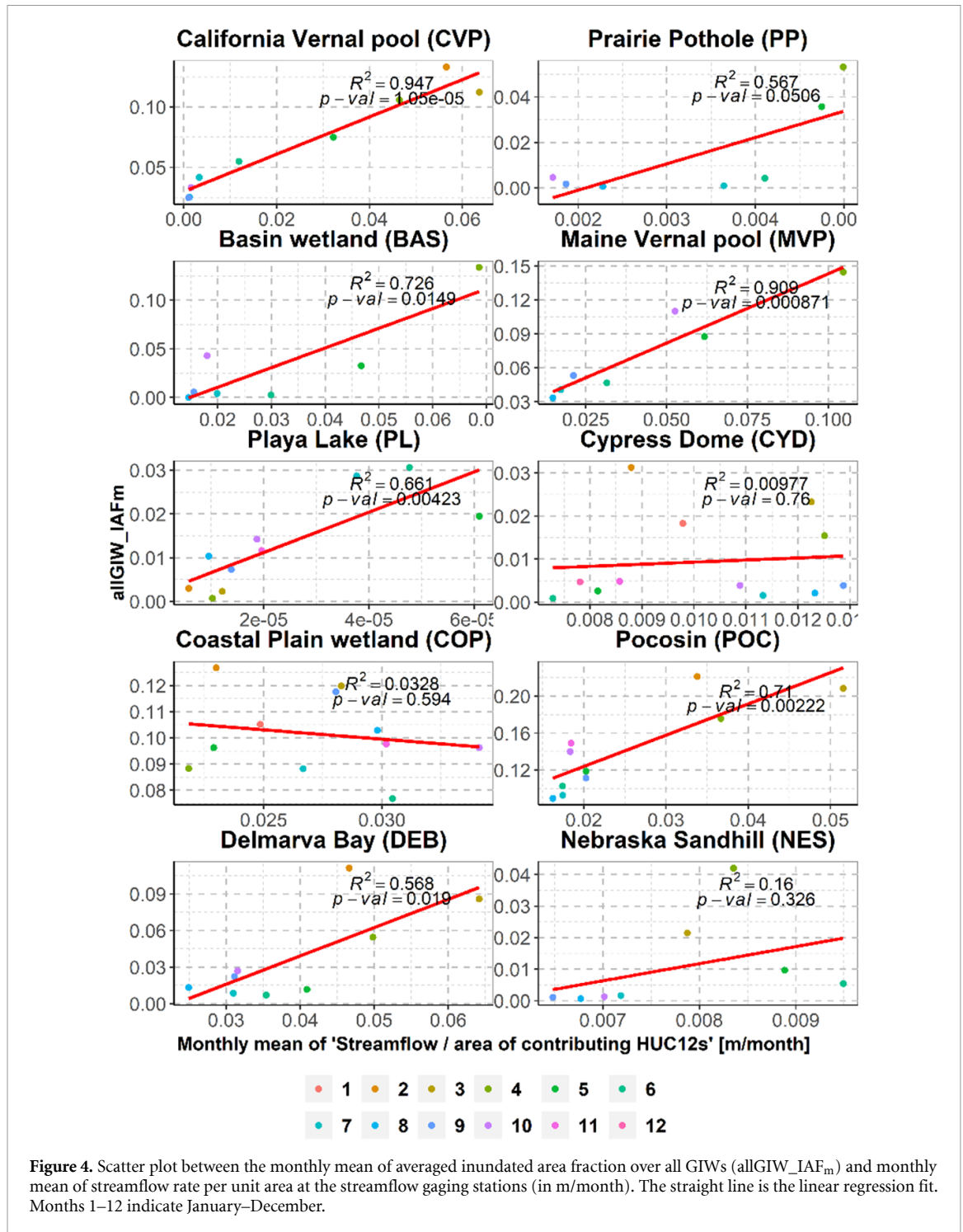## 2.6. Filling gaps in the estimate of mean and std. deviation of GIW inundation area

For certain months and locations, GSW data are non-existent (see figures 1 and S2). Following cues from recent studies (e.g. Walker *et al* 2020) that have demonstrated a correspondence between wetland area and regional water availability descriptors such as streamflow, regressions between inundation characteristics, and monthly streamflows were developed. Here, the allGIW_IAF$_m$ (or allGIW_IAF$_{std}$) for the months with data were considered the response variables. The explanatory variable was the mean monthly streamflow per unit contribution area at a nearby streamflow gaging station. It is to be noted that other meteorological variables such as precipitation (SM + rain) and (precipitation—ET) were also used to generate these relations, but streamflow turned out to be the most explanatory variable overall (see table S2). More information regarding the contribution area of streamflow gaging stations is provided in figures 1, S1 and table S1. Using the regression equations derived in figures 4 and S3, estimates of allGIW_IAF$_m$ (allGIW_IAF$_{std}$) for the months with missing data were obtained. The filling was performed in wetlandscapes CVP, MVP, PL, POC, and DEB. For the wetlandscapes where the regression performance was not satisfactory, i.e. with *p*-value > 0.05 (e.g. wetlandscapes COP and NES), the filling was not performed. As the goal of this study is restricted to assessing the seasonality of wetlands, instead of the exact magnitude of allGIW_IAF$_m$ (or allGIW_IAF$_{std}$), we qualitatively evaluated our overall results with respect to observation data from isolated observations in the considered wetlandscapes. Notably, an alternative regression configuration was also considered. Herein, the response variable was the average inundation fraction of all GIWs for each time step or allGIW_IAF, and the explanatory variable was the corresponding streamflow for these time steps. Results from the analyses indicate that the selected regression configuration (shown in figure 4) is overall more effective than one shown in figure S4 and hence was used for the ensuing analyses.

2.7. Assessing the role of hydroclimatic forcings on inundation seasonality

Inundation dynamics of GIWs are expected to depend on a range of water exchange fluxes (figure S6). GIWs are often recharged by falling rain and snow on them or by the fluxes indirectly supported by rain and SM, such as lateral groundwater flow between wetland and the neighboring aquifer (Neff *et al* 2020, Park *et al* 2020) and runoff from the local contributing area (Shook *et al* 2013, Wang *et al* 2021). Notably, runoff from the contributing area is also a function of rain, SM, and ET . Water is removed from wetlands by open water evaporation, ET via vegetation, and bed leakage (Hayashi *et al* 2003, Shook *et al* 2013, Liu and Kumar 2016). While fine spatio-temporal resolution estimation of these fluxes for each wetland at the scale of our analysis is prohibitive due to lack of refined data and prevalence of a range of processes in play, the overall seasonality is expected to be a function of rain (R), PET, ET, and snowmelt (SM) (Sánchez-Carrillo *et al* 2004, Park *et al* 2014, Penatti *et al* 2015, Liu and Kumar 2016, Zhu *et al* 2017, Bertassello *et al* 2020, Lee *et al* 2020). Here our goal is to assess the extent to which regional data of R, PET, ET, and SM, with inherent uncertainties, can explain the seasonal dynamics of GIW inundation at wetlandscape scale.

To assess the extent to which hydroclimatic forcings influence the seasonal wetland dynamics, multiple linear regression with variable selection was performed at each wetlandscape. The change in allGIW_IAF between consecutive months or allGIW_IAF(t)-allGIW_IAF(t-1) (hereafter ΔallGIW_IAF) was the dependent variable. Here t is the index for a given month. Use of ΔallGIW_IAF, instead of allGIW_IAF, as the dependent variables were driven by the fact that similar allGIW_IAF could be observed within a year during seasonal recharge and recession periods when the meteorological forcings could be very different. The candidate independent variables were R, ET, PET, and

Figure 4. Scatter plot between the monthly mean of averaged inundated area fraction over all GIWs (allGIW_IAF$_m$) and monthly mean of streamflow rate per unit area at the streamflow gaging stations (in m/month). The straight line is the linear regression fit. Months 1–12 indicate January–December.

SM. For the analysis period of *N* years, regressions were generated using different combinations of data of *N-1* years based on the leave-one-out method. All 15 possible subsets of independent variables were considered one-by-one. Among the subsets of independent variables, the subset producing the highest R^2 was selected. This subset was then used to predict ΔallGIW_IAF for the year not considered in the regression. The process was repeated for other *N-1* years. This was followed by evaluation of allGIW_IAF(t) for all months during a year, for every year, using the equation allGIW_IAF(t) = allGIW_IAF(t-1) + ΔallGIW_IAF(t). Predicted allGIW_IAF for all years were then averaged to obtain the seasonality in allGIW_IAF$_m$.

3. Results and discussion

3.1. Seasonality in inundation area of GIWs
Intra-annual variations of IAFs in wetlandscapes are shown in figure 5. Overall, wetlands that are affected by SM (hereafter SM-affected), such as the PP, BAS of Minnesota, MVP, and NES, experienced
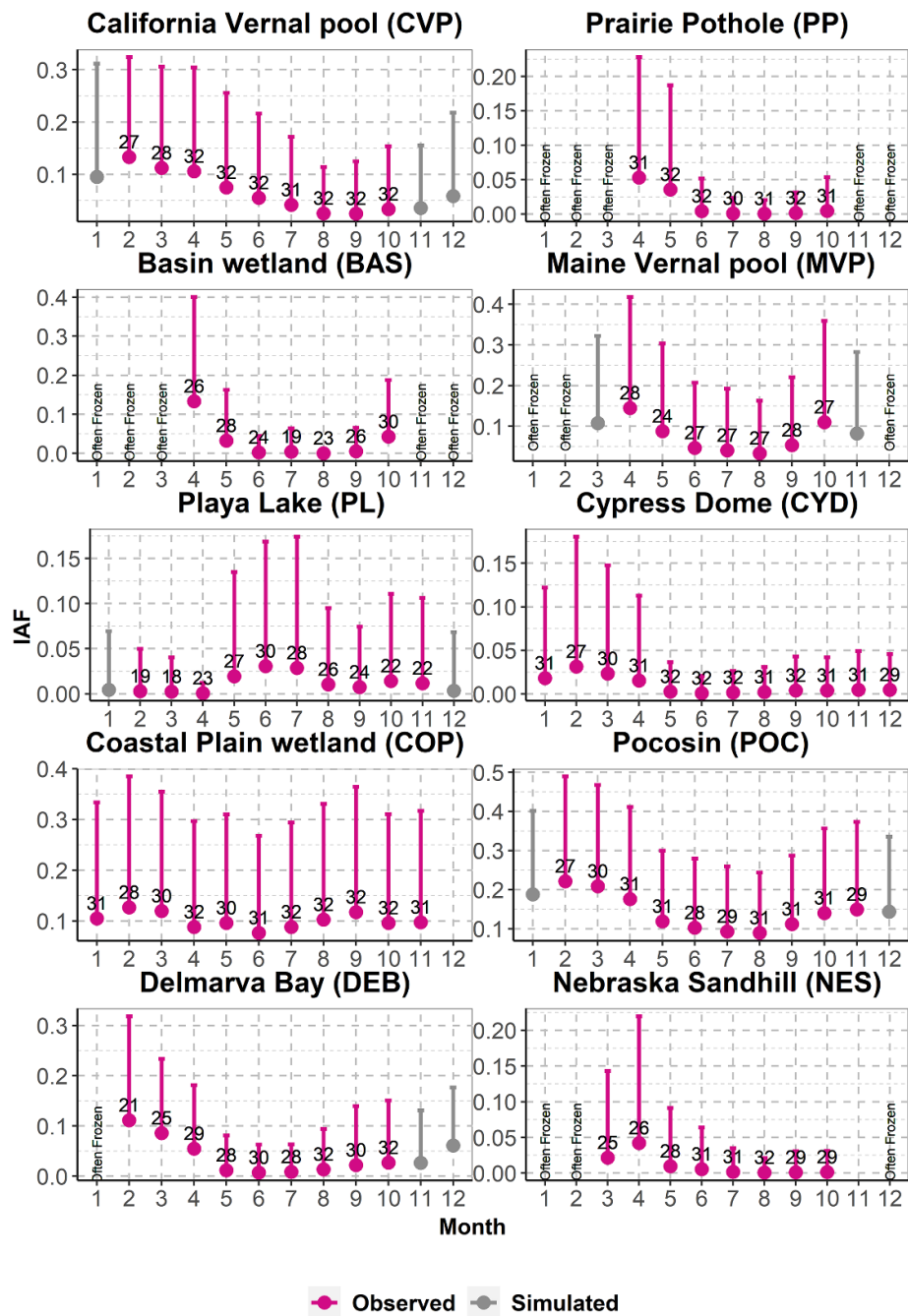
Figure 5. Box plot of monthly averages and standard deviations of IAF. Red dots and whiskers are obtained using observation data. Estimates for months for which data does not exist are shown in grey. These estimates were obtained using the linear regression models shown in figures 4 and S3. Dots indicate monthly averaged inundated area fraction over all GIWs (allGIW_IAF$_m$), and the top extent of whiskers indicate the allGIW_IAF$_m$ + allGIW_IAF$_{std}$. Numbers written above the red dots indicate the number of years for which IAF data is available in the concerned month.

peak allGIW_IAF$_m$ in April. In these wetlandscapes, wetlands may often be frozen in certain winter months. Here the inundation area evaluation is performed only for the months with average air temperature greater than zero in at least 50% of the observation years. It is to be emphasized that the shown temporal variations do not indicate that all GIWs in these wetlandscapes were at their largest inundation extent in April every year, but rather the mean of monthly extents over all GIWs are maximum in April. After April, allGIW_IAF$_m$ progressively decreased till

August. Following August/September, the decreasing trend usually reversed. The extent of intra-annual variations in allGIW_IAF$_m$, however, showed differences across wetlandscapes. For example, compared to the maximum allGIW_IAF$_m$, the minimum allGIW_IAF$_m$ for PP, BAS, MVP, and NES were 1.4%, 0.0%, 23.1%, and 1.6% in magnitude. The coefficient of variation or the ratio of standard deviation to the mean, indicating the magnitude of intra-annual variations of allGIW_IAF$_m$, for these wetlands were 1.46, 1.51, 0.56, and 1.40, respectively. Notably,

intra-annual variation of allGIW_IAF$_m$ in MVP was found to be relatively smaller than in other wetlandscapes. Recovery of the wetland area in fall was also the highest in the MVP, with October allGIW_IAF$_m$ being around 76% of the maximum allGIW_IAF$_m$.

Seasonal variations obtained above, for the most part, align with the groundwater table or water depth variations observed at isolated gaging stations within the concerned wetlandscapes. For example, in the PP region, Johnson *et al* (2004) observed peak water table elevation during April/May and a decrease in the following months. In some years, such as the deluge years of 1994 and 1995 in their observation period, they also reported a second peak in mid-summer or early fall. In most years, the decreasing trend reversed in September/October. It is to be noted that while our results indicate an increase in variability in mid-summer, the data does not show a significant increase in allGIW_IAF$_m$ during this period. Observation sites in BAS and NES also corroborate the overall reported intra-annual variations of allGIW_IAF$_m$ at these wetlandscapes, with peak timing in April followed by a reduction in summer and subsequent recovery in fall. For example, BEC (2010) and MBWSR (2013) reported the highest water table during April/May, a decreasing trend in summer, and recovery in fall in wetlands within Saint Louis and Dodge counties of Minnesota.
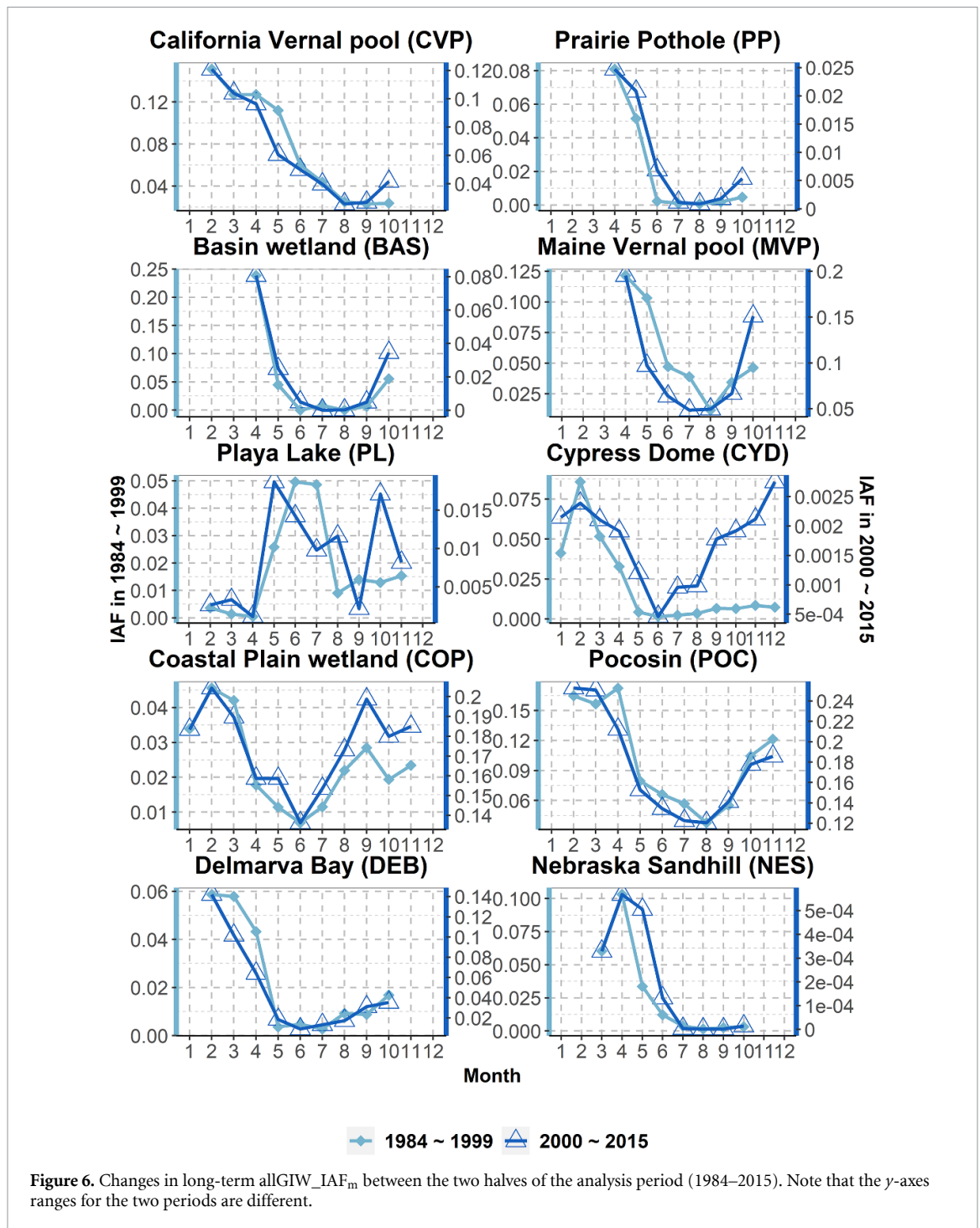
Similarly, Gosselin *et al* (1999) and Gosselin *et al* (2000) observed higher water elevations during March to May within the sandhills of Nebraska. While studies detailing water table dynamics for vernal pools in Maine are scant, its description as 'small, ephemeral wetlands that typically fill in spring with SM and precipitation, or fall with rising water tables, and are dry by summer's end' aligns with the reported temporal variation of inundation area in figure 5 (Calhoun *et al* 2014, p 11 002). Kifner *et al* (2018) also described MVP as 'typically at their highest water level in the spring, dry down by mid-summer, and refill in the autumn, while some dry on cycles longer than a year.'

Among the wetlands that are minimally affected by SM or, in other words, those mostly driven by rain (hereafter rain-fed), the intra-annual variations of inundation were generally similar to each other, but some did show stark differences (figure 5). For example, the allGIW_IAF$_m$ peaked in February in CVP, Florida CYD, COP, POC of North Carolina, and Delmarva bays in Maryland (DEB). In contrast, the peak of allGIW_IAF$_m$ in PL of Texas was in June. Except for PL, all rain-fed wetlandscapes experienced a decrease in allGIW_IAF$_m$ in the months following February, with minimum allGIW_IAF$_m$ usually occurring during May to August. COP and POC showed a second smaller peak during fall, with allGIW_IAF$_m$ magnitude being around 93% and 68% of its maximum value, respectively. In PL, the minimum allGIW_IAF$_m$ usually occurred between February to April. In terms of the extent of variations, the ratio of minimum to maximum allGIW_IAF$_m$ for CVP, CYD, COP, POC, DEB, and PL were 18.7%, 3.1%, 60.6%, 40.4%, 6.5%, and 2.5%, respectively. The coefficient of variation of allGIW_IAF$_m$ for these wetlands were 0.61, 1.07, 0.15, 0.33, 0.99, and 0.82, respectively. The result indicates that the intra-annual variation of the allGIW_IAF$_m$ was relatively moderate in POC and DEB.

Overall, the intra-annual variations in rain-fed wetlands reported in figure 5 align with observations at isolated sites in these wetlandscapes, albeit with a few exceptions. For example, Rains *et al* (2006) observed significant variations in stages in vernal pools following precipitation events, with an overall decreasing trend from February to June. Similarly, Brown (1981) and Kasischke *et al* (2003) reported a water level peak in January in CYD of Florida. Notably, these studies also noted additional isolated peaks between August and October in response to intense precipitation that oftentimes originated from hurricanes or tropical storms. Along the lines of reported results for COP shown in figure 5, Williams *et al* (2002) and Amatya *et al* (2020) observed water table depths in wetlands near the southeastern Atlantic coast peak in spring and autumn and be relatively dry in summer. The distinct seasonality of inundation in PL (see figure 5) is in line with the water depth observations reported by Ganesan (2010) and Weinberg *et al* (2015), where water table peaks were reported in July/August with smaller values in fall and winter.

Overall, during the analyses period, the long-term seasonality or the intra-annual variation of allGIW_IAF$_m$ showed changes in terms of the inundation extent (figure 6). Following the strategy used in Borja *et al* (2020), we divided the analyses period into two halves to track the long-term change. Seasonality was then obtained for both these periods. Eastern CONUS wetlandscapes, including MVP, COP, POC, and DEB, showed an overall increase in wetland extent in the later period. In contrast, western wetlandscapes such as CVP and NES showed an overall decrease in inundation extent. These results are consistent with previously reported open surface water trends (Zou *et al* 2018, Borja *et al* 2020), although it is to be noted that our analyses capture the changes in the inundation extent of the same GIWs over time while the previous studies evaluated the total open surface area over a landscape. This could possibly be the reason why our results show a decrease in inundation, especially during the spring melt, in BAS and PP wetlandscapes, which is in contrast to the results reported in Borja *et al* (2020). Notably, even though the IAFs for these wetlandscapes have changed over time, the dry and wet periods during the year have remained almost the same. For PL, the month with the largest and smallest allGIW_IAF$_m$ shifted by a month.

Figure 6. Changes in long-term allGIW_IAF$_m$ between the two halves of the analysis period (1984–2015). Note that the *y*-axes ranges for the two periods are different.

3.2. Consistency of seasonality in inundated area of GIWs

The previous section discussed the seasonality or the intra-annual variation of allGIW_IAF$_m$ for each wetlandscape. However, as IAF shows significant variations from one year to next (see the monthly mean standard deviation shown in figure 5), it is expected that the maximum (minimum) allGIW_IAF in a given year may not occur in the month with maximum allGIW_IAF$_m$. To assess inter-annual variations in inundation seasonality, its consistency, quantified by the fraction of years the maximum (minimum) allGIW_IAF occurs in the top three

(bottom three) months of allGIW_IAF$_m$, was evaluated. For calculating the consistency, only the years with at least one record among the top three or the bottom three months were used.

In most wetlandscapes, the consistency of month with the maximum inundation area was more than 50% (figure 7), i.e. in more than half of the years, the maximum inundation area lies within the top three months in terms of the magnitude of allGIW_IAF$_m$. For SM-affected wetlandscapes, i.e. PP, BAS, MVP, and NES, corresponding consistencies were all greater than 75%. High consistency in SM-affected wetlands is unsurprising to some extent, as the SM is
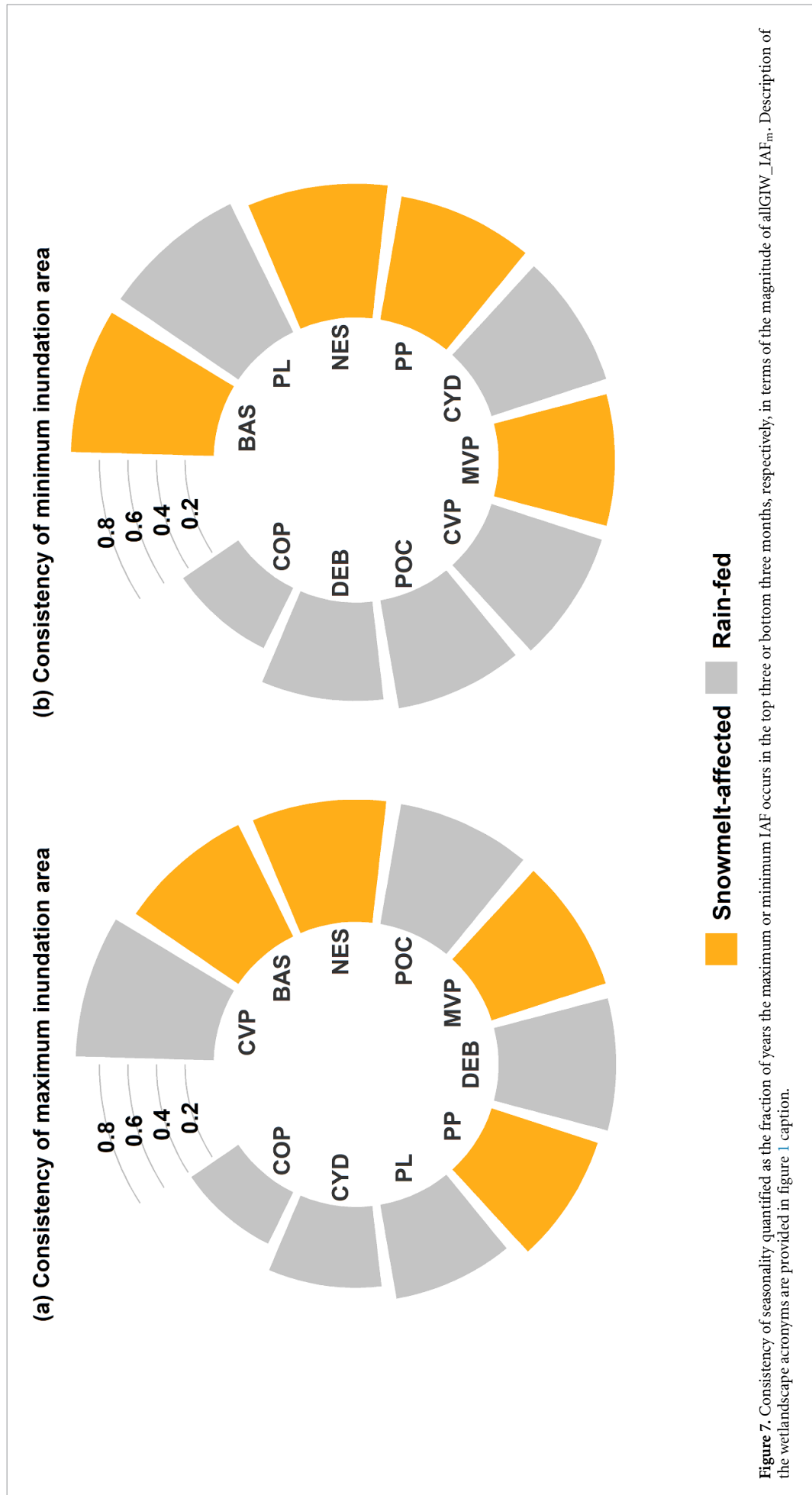
Figure 7. Consistency of seasonality quantified as the fraction of years the maximum or minimum IAF occurs in the top three or bottom three months, respectively, in terms of the magnitude of allGIW_IAF$_m$. Description of the wetlandscape acronyms are provided in figure 1 caption.

dominantly driven by annually recurring higher temperatures and radiation in late spring and early summer. Arguably, an even higher consistency should perhaps be expected for SM-affected wetlandscapes. However, this is not so due to a few large rainfall events in late summer and fall in some of these wetlandscapes, as noted in Neill ([1993](#)) and Johnson *et al* ([2004](#)), which may cause widespread inundation. The consistency of month with the maximum inundation area was relatively smaller for rainfed wetlandscapes CYD and COP, with consistency magnitude being smaller than 50%. Notably, both CYD and COP experience occasional flooding due to hurricanes and/or tropical storms during June to November, thus leading to seasonal peaks in months that do not coincide with the three months with mean maximum allGIW_IAF$_m$. The lower consistency of the month with minimum allGIW_IAF$_m$ for COP can again be partially attributed to these storms. Overall, SM-affected wetlandscapes experience high consistency for the month with minimum allGIW_IAF$_m$, in part due to distinct seasonality of net soil water input that is dominated by SM in late spring/early summer and relatively higher ET rates in summer.

3.3. Hydroclimatic drivers of seasonality

Qualitatively, the monthly variation of both long-term average R + SM and R + SM-ET (see figure S5) shows some correspondence with the intra-annual variation of allGIW_IAF$_m$ (figure [5](#) and table S2). Notably, at least one variable between long-term average R + SM and R + SM-ET with lag of 0 and 1 month shows a coefficient of determination or r^2 value of more than 0.5 in seven out of ten sites. The other three sites where r^2 < 0.5 are CYD, COP, and POC. All of these three sites are affected by rapid inundation due to hurricanes and tropical storms. Overall, R + SM showed better r^2 to allGIW_IAF$_m$ at more sites than R + SM-ET. The aforementioned results indicate that long-term average R + SM and/or R + SM-ET show similar intra-annual variations as allGIW_IAF$_m$ for most sites.

Next, we quantitatively assess the extent to which inundation seasonality can be predicted by the seasonality of controlling fluxes. Here the assessment was performed for the two halves of the analysis period, viz. 1984–1999 and 2000–2015, using the methodology outlined in section [2.7](#). The reason to do the separate assessment for the two periods is that smaller period constraints the extent of anthropogenic change, if any, thus allowing a better understanding of the influence of controlling fluxes on inundation seasonality. Results (figure S8 and table [1](#)) indicate that regressions based on R(t), SM(t), PET(t), and ET(t) can capture more than 52% (57%) of the intra-annual variations in allGIW_IAF$_m$ in 8 out of 10 wetlandscapes during 1984–1999 (2000–2014).

Table 1. Performance of the best multiple linear regression after variable selection using leave-one-out approach (as outlined in section [2.7](#)) between allGIW_IAF$_m$ and monthly averaged ET, PET, R (rainfall), and SM. Description of the wetlandscape acronyms are provided in figure [1](#) caption.

	R^2	
Wetlandscapes	1984–1999	2000–2015
CVP	0.84	0.98
PP	0.90	0.90
BAS	0.52	0.58
MVP	0.93	0.77
PL	0.12	0.46
CYD	0.93	0.86
COP	0.88	0.63
POC	0.37	0.51
DEB	0.83	0.57
NES	0.87	0.85

4. Summary and conclusions

The study evaluated, for the first time, the seasonality of wetland inundation in the major wetlandscapes of the CONUS. This was made possible through the development of an approach to obtain the long-term intra-annual variation of inundation or allGIW_IAF$_m$ in different wetlandscapes, even as the source data of surface inundation had numerous gaps in both space and time. Notably, the approach presented here may be used to map inundation seasonality in alternative wetlandscapes across the globe. Next, the study also evaluated the consistency of intra-annual variations and changes in them during the analyses period. Finally, an assessment of the extent to which the seasonality can be explained based on meteorological fluxes was assessed.

Overall, SM-affected vs. rain-fed wetlandscapes showed a stark difference in the seasonality of inundation. The top three wetlandscape in terms of the coefficient of variation in allGIW_IAF$_m$ were SM affected, indicating large changes in average inundation extent w.r.t. its mean during the year. In contrast, the POC and DEB, both rain-fed wetlands, showed the smallest coefficient of variation in allGIW_IAF$_m$. SM-affected wetlandscapes such as PP, BAS, MVP, and NES are generally found to be maximally inundated during April following spring melt, and then they reduce in the area till August/September when the trend reverses. The derived seasonality is generally found to qualitatively align with observation data from isolated wetlands in the considered wetlandscapes. It is to be noted that some differences in the derived intra-annual variation of allGIW_IAF$_m$ and previously reported variations in water table depth that were observed at isolated wetlands are expected. This is because allGIW_IAF$_m$ provides an aggregated inundation characteristic of multiple wetlands located within 1000 km^2 area over 31 years, while water table depth observations are generally available for

only a few wetlands and that too for a limited period. Another source of discrepancy could be the coarse spatio-temporal resolution of the GSW data, which is only available once a month and at a spatial resolution of 30 m.

Despite the anthropogenic and climatic changes that the considered wetlandscapes may have experienced during the analysis period (1984–2015), they exhibited minimal changes in the timing of dry and wet periods. In terms of the inundation extent, however, contrasting changes in inundation magnitudes were observed. The consistency of the seasonality, a metric to capture the frequency with which the maximum (minimum) inundation occurs in the top three (bottom three) months as defined by long-term averaged inundation area, was generally high in SM-fed wetlands. Even though the rain-fed wetlandscapes are distributed from coast to coast, the majority of them showed remarkable similarity in their seasonality. For example, CVP, CYD, COP, POC, and DEB had the maximum monthly average inundation in February and a minimum during June/August. COP and POC, however, did show a second peak during fall. An exception in seasonality for rain-fed wetlands is the PL, which exhibits maximum monthly inundation in June and minimum during February to April. The inter-annual consistency of the derived seasonality was relatively poor in PL, CYD, and COP, in part due to relatively moderate variations in monthly averaged inundation area across months and the existence of short-burst precipitation events. Overall, widely available data of regional hydroclimatic fluxes were able to explain more than 57% of the seasonality in 7 out of 10 wetlandscapes. The result indicates that despite the numerous hydrologic processes and wetland attributes that determine inundation dynamics, simple multiple linear regressions using widely available meteorological fluxes can capture inundation seasonality at the wetlandscape scale. Similar regressions may be derived for alternative wetlandscapes across the globe, and if they are found to be sufficiently representative across periods, they may be used for assessment of changes in inundation seasonality with changes in climate (Zhu *et al* 2017). These regressions could also be used to fill allGIW_IAF$_m$ estimates for months with insufficient data, as explored in section 2.6.

Although significant care was taken in data analyses, and only GIWs with less than 5% missing data were chosen for analyses, some uncertainty in our conclusions regarding the seasonality could have been introduced by (a) missing GSW data in certain months (see figures 5 and S2), (b) presence of clouds and canopy, (c) use of coarse temporal (once a month) and spatial resolution (30 × 30 m) of the data, (d) inherent uncertainty in the GSW product, (e) presence of barriers that could partition GIWs, (f) uncertainty in regressions that are used to fill mean monthly inundation fraction (allGIW_IAF$_m$)

in months with missing/insufficient data, and (g) undefined date of data capture used to identify inundation pixels. Recent satellite missions such as Sentinel-2 (Wang and Atkinson 2018), WorldView-3 (Pacifici *et al* 2015), SuperView-1 (Kuang *et al* 2018), and those by commercial platforms such as Planet Lab (www.planet.com/) with high-resolution images and advanced quality control processes may help reduce few of these uncertainties to an extent.

Despite the aforementioned challenges, this study, for the first time, maps the seasonality of GIWs, and the changes in it, within the major wetlandscapes of the CONUS using long-term (>30 years) data. In addition, it delineates the inter-annual consistency of the reported seasonality and highlights the role of meteorological controls on them. Given the role of wetlands' inundation on numerous ecosystem services, as outlined in section 1, results of this study and the methods developed herein to map wetland seasonality may be used to assess within-year inundation dynamics' impacts on these services.

Conflict of interest

Authors declare no competing interests.

ORCID iDs

Junehyeong Park ⓘ https://orcid.org/0000-0001-7806-4803
Mukesh Kumar ⓘ https://orcid.org/0000-0001-7114-9978

References

Allen G H and Pavelsky T M 2018 Global extent of rivers and streams *Science* **361** 585–8
Amatya D M, Chescheir G M, Williams T M, Skaggs R W and Tian S 2020 Long-term water table dynamics of forested wetlands: drivers and their effects on wetland hydrology in the southeastern Atlantic coastal plain *Wetlands* **40** 65–79
Baptista J D C, Donnelly T, Rayne D and Davenport R J 2003 Microbial mechanisms of carbon removal in subsurface flow wetlands *Water Sci. Technol.* **48** 127–34

Barr Engineering Co 2010 Wetland hydrology monitoring report 2007–2009 (available at: https://files.dnr.state.mn.us/lands_minerals/northmet/permit_to_mine/wrp/55_barr_2010d.pdf)

Benson C E, Carberry B and Langen T A 2018 Public–private partnership wetland restoration programs benefit species of greatest conservation need and other wetland-associated wildlife *Wetlands Ecol. Manage.* **26** 195–211

Bertasello L E, Rao P S C, Jawitz J W, Aubeneau A F and Botter G 2020 Wetlandscape hydrologic dynamics driven by shallow groundwater and landscape topography *Hydrol. Process.* **34** 1460–74

Bloom A A, Bowman K W, Lee M, Turner A J, Schroeder R, Worden J R, Weidner R, McDonald K C and Jacob D J 2017 A global wetland methane emissions and uncertainty dataset for atmospheric chemical transport models (WetCHARTs version 1.0) *Geosci. Model Dev.* **10** 2141–56

Borja S, Kalantari Z and Destouni G 2020 Global wetting by seasonal surface water over the last decades *Earth's Future* **8** e2019EF001449

Brown S 1981 A comparison of the structure, primary productivity, and transpiration of cypress ecosystems in Florida *Ecol. Monogr.* **51** 403–27

Bullock A and Acreman M 2003 The role of wetlands in the hydrological cycle *Hydrol. Earth Syst. Sci.* **7** 358–89

Calhoun A J K et al 2017 Temporary wetlands: challenges and solutions to conserving a "disappearing" ecosystem *Biol. Conserv.* **211** 3–11

Calhoun A J K, Jansujwicz J S, Bell K P and Hunter M L 2014 Improving management of small natural features on private lands by negotiating the science-policy boundary for Maine vernal pools *Proc. Natl Acad. Sci. USA* **111** 11002–6

Cheng F Y and Basu N B 2017 Biogeochemical hotspots: role of small water bodies in landscape nutrient processing *Water Resour. Res.* **53** 5038–56

Cheng F Y, Van Meter K J, Byrnes D K and Basu N B 2020 Maximizing US nitrate removal through wetland protection and restoration *Nature* **588** 625–30

Cohen M J et al 2016 Do geographically isolated wetlands influence landscape functions? *Proc. Natl Acad. Sci. USA* **113** 1978–86

Creed I F et al 2017 Enhancing protection for vulnerable waters *Nat. Geosci.* **10** 809–15

Freitas J G et al 2019 'Interaction between lakes' surface water and groundwater in the Pantanal wetland, Brazil *Environ. Earth Sci.* **78** 1–15

Ganesan G 2010 Estimating Recharge through Playa Lakes to the Southern High Plains Aquifer *Master Thesis* Texas Tech University

Gilliam J W 1994 Riparian Wetlands and water quality *J. Environ. Qual.* **23** 896

Golden H E et al 2017 Integrating geographically isolated wetlands into land management decisions *Front. Ecol. Environ.* **15** 319–27

Gosselin D C, Drda S, Harvey F E and Goeke J 1999 Hydrologic setting of two interdunal valleys in the central sand hills of Nebraska *Ground Water* **37** 924–33

Gosselin D C, Rundquist D C and McFeeters S K 2000 Remote monitoring of selected ground-water dominated lakes in the Nebraska sand hills *J. Am. Water Resour. Assoc.* **36** 1039–51

Halabisky M, Moskal L M, Gillespie A and Hannam M 2016 Reconstructing semi-arid wetland surface water dynamics through spectral mixture analysis of a time series of Landsat satellite images (1984–2011) *Remote Sens. Environ.* **177** 171–83

Hayashi M, Van Der Kamp G and Schmidt R 2003 Focused infiltration of snowmelt water in partially frozen soil under small depressions *J. Hydrol.* **270** 214–29

Hey D L and Philippi N S 1995 Flood reduction through wetland restoration: the upper Mississippi river basin as a case history *Restor. Ecol.* **3** 4–17

Hill B H, Elonen C M, Herlihy A T, Jicha T M and Serenbetz G 2018 Microbial ecoenzyme stoichiometry, nutrient limitation, and organic matter decomposition in wetlands of the conterminous United States *Wetlands Ecol. Manage.* **26** 425–39

Hird J, DeLancey E, McDermid G and Kariyeva J 2017 Google earth engine, open-access satellite data, and machine learning in support of large-area probabilistic wetland mapping *Remote Sens.* **9** 1315

Holmquist J R et al 2018 Uncertainty in United States coastal wetland greenhouse gas inventorying *Environ. Res. Lett.* **13** 115005

Hondula K L, DeVries B, Jones C N and Palmer M A 2021 Effects of using high resolution satellite-based inundation time series to estimate methane fluxes from forested wetlands *Geophys. Res. Lett.* **48** e2021GL092556

Huang C, Peng Y, Lang M, Yeo I-Y and McCarty G 2014 Wetland inundation mapping and change monitoring using Landsat and airborne LiDAR data *Remote Sens. Environ.* **141** 231–42

Jin H, Huang C, Lang M W, Yeo I-Y and Stehman S V 2017 Monitoring of wetland inundation dynamics in the Delmarva Peninsula using Landsat time-series imagery from 1985 to 2011 *Remote Sens. Environ.* **190** 26–41

Johnson W C et al 2004 Influence of weather extremes on the water levels of glaciated prairie wetlands *Wetlands* **24** 385–98

Jones J 2015 Efficient wetland surface water detection and monitoring via Landsat: comparison with *in situ* data from the everglades depth estimation network *Remote Sens.* **7** 12503–38

Jones J 2019 Improved automated detection of subpixel-scale inundation—revised dynamic surface water extent (DSWE) partial surface water tests *Remote Sens.* **11** 374

Jordan T E, Whigham D F, Hofmockel K H and Pittek M A 2003 Nutrient and sediment removal by a restored wetland receiving agricultural runoff *J. Environ. Qual.* **32** 1534

Kaplan G and Avdan U 2018 Monthly analysis of wetlands dynamics using remote sensing data *ISPRS Int. J. Geo-Inf.* **7** 411

Kasischke E S et al 2003 Effects of seasonal hydrologic patterns in south Florida wetlands on radar backscatter measured from ERS-2 SAR imagery *Remote Sens. Environ.* **88** 423–41

Kayranli B, Scholz M, Mustafa A and Hedmark Å 2010 Carbon storage and fluxes within freshwater wetlands: a critical review *Wetlands* **30** 111–24

Kifner L H, Calhoun A J K, Norton S A, Hoffmann K E and Amirbahman A 2018 Methane and carbon dioxide dynamics within four vernal pools in Maine, USA *Biogeochemistry* **139** 275–91

Knight R L, Clarke R A and Bastian R K 2001 Surface flow (SF) treatment wetlands as a habitat for wildlife and humans *Water Sci. Technol.* **44** 27–37

Krapu C, Kumar M and Borsuk M 2018 Identifying Wetland consolidation using remote sensing in the North Dakota Prairie Pothole Region *Water Resour. Res.* **54** 7478–94

Kuang J et al 2018 Coseismic deformation and source model of the 12 November 2017 MW 7.3 Kermanshah earthquake (Iran–Iraq border) investigated through DInSAR measurements *Int. J. Remote Sens.* **40** 532–54

Lane C R and D'Amico E 2010 Calculating the ecosystem service of water storage in isolated wetlands using LiDAR in north central Florida, USA *Wetlands* **30** 967–77

Lane C R and D'Amico E 2016 Identification of putative geographically isolated Wetlands of the conterminous United States *J. Am. Water Resour. Assoc.* **52** 705–22

Lane C R, Leibowitz S G, Autrey B C, LeDuc S D and Alexander L C 2018 Hydrological, physical, and chemical functions and connectivity of non-floodplain wetlands to downstream waters: a review *J. Am. Water Resour. Assoc.* **54** 346–71

Lee S et al 2020 Seasonal drivers of geographically isolated wetland hydrology in a low-gradient, Coastal Plain landscape *J. Hydrol.* **583** 124608

Lin Y-F, Jing S-R, Wang T-W and Lee D-Y 2002 Effects of macrophytes and external carbon sources on nitrate removal

from groundwater in constructed wetlands *Environ. Pollut.* **119** 413–20

Liu T, Xu S, Lu S, Qin P, Bi B, Ding H, Liu Y, Guo X and Liu X 2019 A review on removal of organophosphorus pesticides in constructed wetland: performance, mechanism and influencing factors *Sci. Total Environ.* **651** 2247–68

Liu Y and Kumar M 2016 Role of meteorological controls on interannual variations in wet-period characteristics of wetlands *Water Resour. Res.* **52** 5056–74

Luijendijk A *et al* 2018 The state of the world's beaches *Sci. Rep.* **8** 1–11

Luo L *et al* 2003 Validation of the North American land data assimilation system (NLDAS) retrospective forcing over the southern Great Plains *J. Geophys. Res. Atmos.* **108** 8843

Marchand L, Mench M, Jacob D L and Otte M L 2010 Metal and metalloid removal in constructed wetlands, with emphasis on the importance of plants and standardized measurements: a review *Environ. Pollut.* **158** 3447–61

Marton J M *et al* 2015 Geographically isolated Wetlands are important biogeochemical reactors on the landscape *BioScience* **65** 408–18

Maxwell R M, Condon L E and Kollet S J 2015 A high-resolution simulation of groundwater and surface water over most of the continental US with the integrated hydrologic model ParFlow v3 *Geosci. Model Dev.* **8** 923–37

McCarthy T S 2006 Groundwater in the wetlands of the Okavango Delta, Botswana, and its contribution to the structure and function of the ecosystem *J. Hydrol.* **320** 264–82

Melton J R *et al* 2013 Present state of global wetland extent and wetland methane modelling: conclusions from a model inter-comparison project (WETCHIMP) *Biogeosciences* **10** 753–88

Mentaschi L, Vousdoukas M I, Pekel J-F, Voukouvalas E and Feyen L 2018 Global long-term observations of coastal erosion and accretion *Sci. Rep.* **8** 12876

Minnesota Board of Water and Soil Resources 2013 *Hydrologic Monitoring of Wetlands—MN Board of Water & Soil Resources Supplemental Guidance* (Saint Paul, MN: Minnesota Board of Water and Soil Resources)

Mitchell K E *et al* 2004 The multi-institution North American land data assimilation system (NLDAS): utilizing multiple GCIP products and partners in a continental distributed hydrological modeling system *J. Geophys. Res. Atmos.* **109** D07S90

Mitsch W J and Gosselink J G 2000 The value of wetlands: importance of scale and landscape setting *Ecol. Econ.* **35** 25–33

Mungur A S *et al* 1995 An assessment of metal removal from highway runoff by a natural wetland *Water Sci. Technol.* **32** 169–75

Mushet D M *et al* 2015 Geographically isolated wetlands: rethinking a misnomer *Wetlands* **35** 423–31

Nan Z *et al* 2010 Analysis of spatial similarities between NEXRAD and NLDAS precipitation data products *IEEE J. Sel. Top. Appl. Earth Obs. Remote Sens.* **3** 371–85

Nearing G S *et al* 2016 Benchmarking NLDAS-2 soil moisture and evapotranspiration to separate uncertainty contributions *J. Hydrometeorol.* **17** 745–59

Neff B P *et al* 2020 A hydrologic landscapes perspective on groundwater connectivity of depressional wetlands *Water* **12** 50

Neill C 1993 Seasonal flooding, soil salinity and primary production in northern prairie marshes *Oecologia* **95** 499–505

Pacifici F *et al* 2015 Measuring the spatial and spectral performance of WorldView-3 *Fourier Transform Spectroscopy and Hyperspectral Imaging and Sounding of the Environment* (Optical Society of America) p HW3B.2

Pan M *et al* 2003 Snow process modeling in the North American land data assimilation system (NLDAS): 2. Evaluation of model simulated snow water equivalent *J. Geophys. Res. Atmos.* **108** 8850

Park J *et al* 2014 Stochastic modeling of hydrologic variability of geographically isolated wetlands: effects of hydro-climatic forcing and wetland bathymetry *Adv. Water Resour.* **69** 38–48

Park J, Wang D and Kumar M 2020 Spatial and temporal variations in the groundwater contributing areas of inland wetlands *Hydrol. Process.* **34** 1117–30

Pekel J-F, Cottam A, Gorelick N and Belward A S 2016 High-resolution mapping of global surface water and its long-term changes *Nature* **540** 418–22

Penatti N C *et al* 2015 Satellite-based hydrological dynamics of the world's largest continuous wetland *Remote Sens. Environ.* **170** 1–13

Rains M C *et al* 2006 The role of perched aquifers in hydrological connectivity and biogeochemical processes in vernal pool landscapes, Central Valley, California *Hydrol. Process.* **20** 1157–75

Reuter J E, Djohan T and Goldman C R 1992 The use of wetlands for nutrient removal from surface runoff in a cold climate region of California—results from a newly constructed wetland at lake tahoe *J. Environ. Manage.* **36** 35–53

Rezaee M *et al* 2018 Deep convolutional neural network for complex wetland classification using optical remote sensing imagery *IEEE J. Sel. Top. Appl. Earth Obs. Remote Sens.* **11** 3030–9

Sánchez-Carrillo S *et al* 2004 Evapotranspiration in semi-arid wetlands: relationships between inundation and the macrophyte-cover: open-waterratio *Adv. Water Resour.* **27** 643–55

Sarkar D J *et al* 2021 Occurrence, fate and removal of microplastics as heavy metal vector in natural wastewater treatment wetland system *Water Res.* **192** 116853

Sawatzky M E and Fahrig L 2019 Wetland buffers are no substitute for landscape-scale conservation *Ecosphere* **10** e02661

Schück M and Greger M 2020 Plant traits related to the heavy metal removal capacities of wetland plants *Int. J. Phytoremediation* **22** 427–35

Shook K, Pomeroy J W, Spence C and Boychuk L 2013 Storage dynamics simulations in prairie wetland hydrology models: evaluation and parameterization *Hydrol. Process.* **27** 1875–89

Thorslund J *et al* 2017 Wetlands as large-scale nature-based solutions: status and challenges for research, engineering and management *Ecol. Eng.* **108** 489–97

Tiner R W 1997 NWI maps: what they tell us *Natl Wetlands Newsletter* **19** 7–12 (available at: www.fws.gov/wetlands/ Documents/NWI-Maps-What-They-Tell-Us.pdf)

Tiner R W 2003a Estimated extent of geographically isolated wetlands in selected areas of the United States *Wetlands* **23** 636–52

Tiner R W 2003b Geographically isolated wetlands of the United States *Wetlands* **23** 494–516

U.S. Fish and Wildlife Service 2019 National wetlands inventory (available at: www.fws.gov/wetlands/) (Accessed 20 April 2019)

Van Meter K J and Basu N B 2015 Signatures of human impact: size distributions and spatial organization of wetlands in the Prairie Pothole landscape *Ecol. Appl.* **25** 451–65

Walker J J, Soulard C E and Petrakis R E 2020 Integrating stream gage data and Landsat imagery to complete time-series of surface water extents in Central Valley, California *Int. J. Appl. Earth Obs. Geoinf.* **84** 101973

Wang D, Liu Y and Kumar M 2018 Using nested discretization for a detailed yet computationally efficient simulation of local hydrology in a distributed hydrologic model *Sci. Rep.* **8** 1–11

Wang N, Chu X and Zhang X 2021 Functionalities of surface depressions in runoff routing and hydrologic connectivity modeling *J. Hydrol.* **593** 125870

Wang Q *et al* 2019 Enhancement of COD removal in constructed wetlands treating saline wastewater: intertidal wetland sediment as a novel inoculation *J. Environ. Manage.* **249** 109398

Wang Q and Atkinson P M 2018 Spatio-temporal fusion for daily Sentinel-2 images *Remote Sens. Environ.* **204** 31–42

Watson K B *et al* 2016 Quantifying flood mitigation services: the economic value of otter creek wetlands and floodplains to Middlebury, VT *Ecol. Econ.* **130** 16–24

Weinberg P G A, Backhouse S and Gitz D 2015 *Technical Note 15-03 A Water Resource Assessment of the Playa Lakes of the Texas High Plains* (Lubbock, TX: Texas Water Development Board)

Williams R K *et al* 2002 *Management of South Atalantic Coastal Wetlands for Waterfowl and Other Wildlife* (Memphis, TN: Ducks Unlimited)

Wossenyeleh B K *et al* 2021 Drought propagation and its impact on groundwater hydrology of wetlands: a case study on the Doode Bemde nature reserve (Belgium) *Nat. Hazards Earth Syst. Sci.* **21** 39–51

Wu Q *et al* 2019 Integrating LiDAR data and multi-temporal aerial imagery to map wetland inundation dynamics using Google Earth engine *Remote Sens. Environ.* **228** 1–13

Wu Q and Lane C R 2016 Delineation and quantification of wetland depressions in the prairie pothole region of North Dakota *Wetlands* **36** 215–27

Wu Q and Lane C R 2017 Delineating wetland catchments and modeling hydrologic connectivity using lidar data and aerial imagery *Hydrol. Earth Syst. Sci.* **21** 3579–95

Xia Y *et al* 2012 Continental-scale water and energy flux analysis and validation for the North American land data assimilation system project phase 2 (NLDAS-2): 1. Intercomparison and application of model products *J. Geophys. Res. Atmos.* **117** D03109

Yu X, Bhatt G, Duffy C and Shi Y 2013 Parameterization for distributed watershed modeling using national data and evolutionary algorithm *Comput. Geosci.* **58** 80–90

Zedler J B and Kercher S 2005 Wetland resources: status, trends, ecosystem services, and restorability *Annu. Rev. Environ. Resour.* **30** 39–74

Zhang Y, Li W, Sun G and King J S 2019 Coastal wetland resilience to climate variability: a hydrologic perspective *J. Hydrol.* **568** 275–84

Zhang Z *et al* 2017 Emerging role of wetland methane emissions in driving 21st century climate change *Proc. Natl Acad. Sci. USA* **114** 9647–52

Zhu J *et al* 2017 Modeling the potential impacts of climate change on the water table level of selected forested wetlands in the southeastern United States *Hydrol. Earth Syst. Sci.* **21** 6289–305

Zou Z *et al* 2018 Divergent trends of open-surface water body area in the contiguous United States from 1984 to 2016 *Proc. Natl Acad. Sci. USA* **115** 3810–5